VON KARMAN INSTITUTE FOR FLUID DYNAMICS

LECTURE SERIES 1987-03

INFLUENCE OF ENVIRONMENTAL FACTORS ON AIRCRAFT WING PERFORMANCE

FEBRUARY 16 - 20, 1987

THE POTENTIAL INFLUENCE OF RAIN ON AIRFOIL PERFORMANCE

R. EARL DUNHAM, JR

NASA LANGLEY RESEARCH CENTER, USA

THE POTENTIAL INFLUENCE OF RAIN ON AIRFOIL PERFORMANCE

by

R. Earl Dunham, Jr.
NASA Langley Research Center
Hampton, Virginia 23665

Lecture Presented at the
von Karman Institute for Fluid Dynamics
Lecture Series Entitled
"Influence of Environmental Factors on Aircraft Wing Performance"
February 1987

Introduction

Around 1970, attention began to focus on the effect of low altitude wind shears and the hazard they present to airplanes. Wind shears have since become a recognized hazard and concerted efforts are underway to provide warning, guidance, and operating procedures for avoiding and escaping serious wind shear threats. Recently, attention has been given to the possible effects of rain on airfoil performance and the effect of rain-induced performance degradation during a simultaneous wind shear encounter.

The effects of finite roughness elements, frost accumulation, and icing on single- and multi-element airfoil performance has long been recognized, but until recently little attention has been directed at the influence of rain. The influence of rain on airfoil performance has long been thought to be insignificant, although the potential for rain to act as a contaminant on an airfoil surface is generally recognized. The primary hazards associated with airplane operations in rain were generally considered to result from a loss of visual reference. In considering rain effects, the basic fluid mechanics problem to be addressed is the generation of lift in a two-component, two-phase (water-air), low-quality flow. Low quality in the fluid dynamic sense refers to one component representing a very small percent of the total mass flow. The details of the deposition of water on the airfoil, the formation of a water layer, the movement of the water over the airfoil, and the interaction of the water with the general airflow around the airfoil and in the boundary layer all determine the aerodynamic characteristics of the airfoil.

This paper is an overview of the most recent work conducted by NASA and others to study the potential influences of heavy rain on airfoil performance. The overview includes a discussion of some of the previous analytical investigations of rain effects on airfoils, reviews some promising experimental methods for evaluating rain effects, and presents some important scaling considerations for extrapolating model data. The latest experimental results are also presented and discussed. At this time a complete understanding of the influence of rain on airfoil aerodynamics is very elusive, and considerable additional effort, both analytically and experimentally, is required to understand the degree of hazard associated with flight operations in a rain environment. It is hoped that this paper will serve to stimulate additional research in this important area.

Properties of Rain

In order to develop analytical models of the effect of rain on airfoil performance and to conduct experimental studies, the phenomenon of naturally occuring precipitation needs to be understood. Two "lump parameter" quantities generally used to describe rain are rainfall rate (R) and liquid water content (LWC). Rainfall rate is a linear accumulation depth at ground level per unit time, and the liquid water content is the mass of liquid water per unit volume, usually expressed as gm/m^3. In the abscence of a vertical wind velocity, the LWC is directly related to the rainfall rate. An additional important parameter for quantifying rain is the rain drop size distribution. An understanding of this distribution is required for experimentally and analytically modeling rain. An understanding of frequency of occurrence and range of rain rate is also required in order to assess hazard potential for aircraft operation .

In 1947 Marshal and Palmer (reference 1) collected data which showed that the size distribution of rain in a cloud could be estimated using an exponential expression of the form:

$$N(D) = N_0 e^{-ID} \qquad (1)$$

where N(D) is the drop size distribution (density function) in terms of the number of drops per cubic meter of air per unit interval, D is the drop diameter, and $I = nR^m$ where n, m, and N_0 are empirically determined constants and R is rainfall rate. Data from Marshall and Palmer indicated that $N_0 = 8000$, $n = 4.1$, and $m = -.21$ for light continuous rain. More recent studies (references 2 and 3) have shown that the values of N_0, n, and m are dependent upon storm type and intensity. Reference 2, for example, suggests that the distribution in heavy thunderstorm-type rain is best characterized by $N_0 = 1400$, $n = 3.0$, and $m = -.21$.

The drop size distribution is used to determine the liquid water content as a function of rain rate. The liquid water content is the integrated sum of the mass of each drop multiplied by the number of drops of each size per unit volume as follows:

$$LWC = \int_0^\infty \rho_w \frac{\pi}{6} D^3 N(D)\, dD$$

where: ρ_w = density of water

When the integration is performed this expression becomes:

$$LWC = \frac{N_0 \rho_w \pi}{I^4}$$

Substituting $I = nR^m$

then: $$LWC = \frac{N_0 \rho_w \pi}{n^4 R^{4m}} \qquad (2)$$

Using the aforementioned expression for the drop size distribution for thunderstorm-type rain, the liquid water content in gm/m^3 is related to rainfall rate by:

$$LWC = \frac{1400 \pi 10^{-3}}{3^4 R^{-.84}} = .054 R^{.84} \qquad (3)$$

Substituting the expression for drop size distribution for the light widespread rain into equation (2), the equation for LWC in terms of rainfall rate becomes:

$$LWC = \frac{8000 \pi 10^{-3}}{4.1^4 R^{-.84}} = .08894 R^{.84} \qquad (4)$$

Figure 1 is a plot of the LWC as a function of rainfall rate for both light widespread rain and thunderstorm type rain. Rain is adequately modeled by equations (1), (3), and (4) when the type of rain environment is specified (thunderstorm or continuous) and either the liquid water content or rainfall rate is given.

The range of rain rates that an airplane could expect to encounter varies from light rain of 5-10 mm per hour up to very large rain rates, the upper boundary currently being the measured world record rain fall rate of 1874 mm/hr. (reference 4). This rate was measured in an intense afternoon thunderstorm on July 4, 1956. For this world record the total storm precipitation was 3.6 inches which fell during a 50 minute period. The rainfall was measured with a recording rain gage at a Maryland state climotology site at Unionville, Maryland, and exceeded the previous record by 830 mm/hr.

For determining the potential for encountering a given rainfall rate the probability distribution data collected by Jones and Sims (reference 5) are useful. They analyzed data collected over a one-year period on recording raingages placed throughout the world. Gages from maritime subtropical, continential temperate, maritime temperate, and midlatitude interior regions were used. The frequency distribution for rainfall rate was obtained at stations in these climate zones, and an average zonal frequency distribution was calculated for each climate zone. These distributions are shown in figure 2. The most intense rainfalls were recorded at stations in the maritime subtropical zone which encompasses the entire southeastern and Gulf coastal regions of the United States. The curves shown in figure 2 cover the range from the recording sensitivity of the gage (.25mm/hr.) to the maximum recorded rate in the one-year sample (238 mm/hr). The probable number of minutes a given rainfall rate (or greater) can be expected in a given climatological zone can be obtained from figure 2 by converting the ordinate from percent to a fractional portion of the time and multiplying by 5.2596×10^5 (the number of minutes in a year). For about two minutes every year in the maritime subtropical zone, a rainfall rate of greater than 200 mm/hr could be expected at any location. Higher rainfall rates from 200 mm/hr to near record rainfall rates have lower probabilities of occurrence.

The results of Jones and Sims are based on ground-level recorded data, but measurements made above ground level by airplanes instrumented for atmospheric research have shown that significantly higher concentrations of liquid water can be found inside thunderstorms (reference 6). These locations are probably in convergence regions of the storm. The work of Roys and Kessler inside high-plains thunderstorms, for example, showed average values of LWC of 8.7 gm/m^3 with a peak valve of 44 gm/m^3. These in-cloud measured liquid water contents, when converted to rainfall rate by the use of equation (3), yield rain rates of 400 mm/hr. and 2920 mm/hr, respectively. Radar measurements of these storms indicated considerably lower expected ground-level rain rates. The data of reference 6 therefore indicate that the probablity of an airplane encountering rainfall rates greater than 200 mm/hr at altitude may be higher than the probability indicated by the ground-level measured data of reference 5.

Analytical Efforts

The computation of airfoil performance, including viscous effects near stall, is by no means a mature technology, and it is even more uncertain in a rain environment where these computations must be made for a two-component, two-phase flow field. An idealization of rain drops interacting with an airfoil is shown in figure 3. Drop interactions include drop trajectories with respect to streamlines, drop splash-back ejecta in regions of near oblique drop encounters, and splash-back ejecta coupled with water film "runback" interaction with the air boundary layer. Gaining a detailed understanding of the physical phenomena and developing an accurate mathematical model poses

a unique aerodynamic challenge which has not yet been accomplished, although several efforts have been directed at describing certain aspects of the problem.

One of the first efforts to estimate the possible performance decrement on an airplane during an encounter with heavy rain was done by Rhode in 1941 (reference 7). In that study, he calculated the drag increase on a DC-3 airplane encountering a rain cloud with a liquid water content of 50 gm/m^3 by considering the momentum imparted to the airplane by the impacting rain drops. His results showed a drag increase which caused about an 18 percent reduction in airspeed. Rhode considered such an encounter to be of a short duration and of little consequence to an airplane flying at 5000 ft. Since low visibility landings and take-offs were not routine in 1941, the consequence of a heavy rain encounter during landing and take-off was not considered.

Since Rhode's effort, the subject of the influence of rain on airplane performance was not addressed again until 1982 when Haines and Luers conducted the study of reference 8. In the time intervening between 1941 and 1982 considerable work had been done to calculate the motion of water drop particles in the flow field about an airfoil, but those studies were primarily aimed at icing cloud droplets. Noteable works in this area were done by Bergmen in 1947 and 1952 (reference 9 and 10), Derch and Brun in 1953 (reference 11), Morsi and Alexander in 1972 (reference 12), and more recently by Bragg in 1982 (reference 13). These efforts were directed at calculating water drop trajectories and impingement on the airfoil for estimating regions of ice accretion and the influence of liquid water on the airfoil performance was not calculated. The governing equations and relationships described in these studies can, however, be used to calculate rain drop trajectories if the drop sizes are increased from icing cloud droplet sizes of 10 to 100 microns to rain drop sizes of 500 to 6000 microns.

The Haines and Luers effort was the first attempt at refining the 1941 study of Rhode to estimate the effects of rain on modern-day airplanes. In addition to including the impact momentum of the rain drops in a similar fashion as Rhode, Haines and Luers included estimates of skin friction roughness effects due to a wavy water layer which was roughened by rain drop impact craters on the surface. The skin friction drag increase was calculated by equating the water layer waviness and rain drop impact crater effects to an equivalent sand grain roughness. Calculated drag increases for a 747 airplane ranged from 2 to 5 percent for rainfall rates from 100 to 1000 mm/hr. Haines and Luers also hypothesized that if rain increased the surface roughness it probably caused effects on an airfoil similar to those of frost or ice including a decrease in the maximum lift capability and a decrease the stall angle. Using empirical estimates of roughness effects on airfoil lift they calculated the rain effect on lift and estimated reductions in the maximum lift of 7 to 29 percent with associated reductions in stall angle from 1 to 5 degrees for rainfall rates from 100 to 1000 mm/hr.

In 1984 Calarese and Hankey (reference 14) studied rain effects by considering the droplet drag acting as a body force in the Navier-Stokes equations. Such an analysis neglects the interface effects of droplet splashing, cratering, and water layer formation. Their analysis produced pressure distribution calculations for a NACA 0012 airfoil for the limiting cases of a very fine rain (small drop size and drop Reynolds number much less than 1) and for a coarse rain (large drop size and drop Reynolds number). For the case of coarse rain, little variation in airfoil pressure distribution was noted. For the limiting case of a fine rain, appreciable changes in calculated pressure distribution were obtained and showed a small linear increase in lift with increasing water spray concentration.

In 1985, Kisielewski (reference 15) performed a three-dimensional Euler analysis to investigate the effect of momentum and energy exchange between the rain and the flow field. He concluded that the rain had little effect on the calculated lift produced by a simple airfoil. The authors of references 14 and 15 concluded that the major influence of rain on airfoil performance was probably dominated by viscous effects of the water droplet splashing and its subsequent interaction with the air boundary layer, but these effects were not modeled in their analysis.

Experimental Methods

The experimental investigation of rain effects on the aerodynamics of airplanes is a technical challenge as difficult as investigating the effects analytically. A full-scale flight test investigation would require that performance measurements be made on an airplane while in a severe rain storm. The test airplane, besides being instrumented for aerodynamic performance measurements, must be equipped to document the meterological environment. The test pilot's task would be to explore the operating envelope up to and including stall while in instrument flight conditions. The tests would probably be conducted in a strong wind and turbulence environment making the extraction of accurate performance parameters very difficult. Additionally, because of the variability of natural rain, repeatable conditions would be difficult if not altogether impossible to obtain.

Small-scale model tests of the effects of rain presents a different set of challenges than flight tests in that they require the simulation of rain and a knowledge of scaling laws for extrapolation of results. The three types of facilities which have so far been used for investigating rain effects are (1) a rotating arm in which a model is placed at the end of a

counterbalanced rotating beam, (2) a model towing facility in which the model is translated down a straight track segment, and (3) conventional wind tunnels.

Rotating arm facilities have been quite useful for studying single-drop impact dynamics (reference 16). Airfoil performance measurements have not been attempted with the rotating-arm facility because the centrifugal effects on the water film would influence the results. Wind tunnels and towing facilities are considered to be the best methods of obtaining airfoil performance data, and in both of these methods the technique for simulating rain and developing scaling relationships presents the area of greatest difficulty. For the model towing facility the water manifolding and nozzle distribution becomes quite elaborate and extensive in order to cover the test area. For the wind tunnel, the difficulty lies in obtaining a uniform distribution of the water with a minimum of influence on the tunnel flow conditions.

The majority of rain effects data to date have been obtained in wind tunnel tests. The tests generally involve placing a spray distribution system upstream of a model and directing the spray at the model while conventional force measurements are obtained (figure 4). Since most of the data presented in this paper were collected in the National Aeronautics and Space Administration's Langley Research Center 14- by 22-Foot Subsonic Tunnel, the spray system used in that facility will be discussed here. Differences in the spray system for data other than those obtained in the 14- by 22-Foot Subsonic Tunnel are noted.

The spray manifold (figure 5) used in the 14- by 22-Foot Subsonic Tunnel consisted of streamline tubing having a streamwise dimension of 3.5 inches and a fineness ratio of 2.2. A remotely controlled, air-pressure-regulated water supply system was connected to the manifold, and variations in the air pressure were used to control volumetric flow through the manifold. Volumetric flow and supply pressure were both measured and recorded. The manifold was configured to receive spray nozzles at 6-inch increments along its trailing edge. The optimization of nozzle location for uniform spray distribution and desired spray coverage was done by trial and error for each different model configuration.

The spray nozzles used in the tests are shown in Figure 6. One nozzle was a commercially available fan jet configuration, and the other nozzle consisted of a series of tubes oriented circumferentially around a central plenum. For the purposes of our test program, the second nozzle was found to be quite adaptable in its ability to vary spray characteristics. Spray drop size and number density could be controlled easily by changing the size and members of tubes. For this series of tests, five-tube and seven-tube configurations were used. The inside tube diameter for both configurations was 0.063 inches.

The spray characteristics were quantified in terms of liquid water content, drop size distribution, and drop velocity. The liquid water content was determined as illustrated in figure 7 by determining the cross-sectional area of spray coverage and volumetric flow in the manifold system. The area coverage was obtained just in front of the wing model by photographing the spray width and height. The photographic qualities of spray were enhanced by using a flourescent dye and ultraviolet strobe light.

Drop size and distribution were obtained from a shadowgraph using a pulsed Doppler laser as an illumination source. The set-up as illustrated in figure 7 used a 1 joule, 20 nsec pulsed ruby laser. The photographic optics were setup to examine a small region in the central part of the spray. The photographic negatives (figure 9) were digitized on a computerized optical scanner and analyzed to determine drop population characteristics. The laser system was also operated in a double pulsed mode of about 20μsec between pulses. This mode allowed for the determination of drop velocity. For the nozzles used the median drop size was from .5 to 1.5 mm, depending on tunnel speed, and the drop velocity at the model was within about 10% of the freestream air velocity. Some additional details of this spray calibration procedure are available in reference 17.

The water spray manifold and the spray cloud alter the wind tunnel flow condition slightly. In particular, an increased free-stream turbulence level is to be expected. It should be noted that, since the density of air is 1100 gm/m^3, even at the large liquid water content concentration (40 to 60 gm/m^3), the water represents a small percent of the total mass flow. The water is injected by the nozzles at slightly below the freestream velocity and is accelerated nearly to freestream velocity by droplet drag. This acceleration does reduce the air stream momentum slightly. The net result is that the tunnel dynamic pressure, with which force measurements are nondimensionalized, remains essentially unchanged since the freestream density in increased slightly to offset the small velocity decrease. In the 14- by 22-Foot Subsonic Tunnel, pitot-static measurements were made with and without the spray and no change in dynamic pressure was measured.

Scaling Analysis

In 1985, Bilanin (reference 18) addressed the subject of scaling for model tests of airfoils under simulated heavy rainfall, and the important findings of that analysis are summarized here. The complexity of the scaling problem was reduced by an analysis which indicated that thermodynamic effects of condensation and evaporation would make a small change in lift curve slope (less than 3%) even for very heavy rainfalls. By ignoring these thermodynamic effects, the scaling problem could be treated as illustrated in figure 3 where a subsonic airfoil is operated in a two-component

flow field. The actual surface of the airfoil is assumed to be smooth so that surface roughness is not a parameter.

The dimensional variables which control the aerodynamic force F generated on the airfoil are:

	Variable	Units
ρ_a	density of air	ML^{-3}
ρ_w	density of water	ML^{-3}
γ_a	kinematic viscosity of air	L^2T^{-1}
γ_w	kinematic viscosity of water	L^2T^{-1}
$\sigma_{w,a}$	surface tension water-air	MT^{-2}
$\sigma_{w,s}$	surface tension water-solid	MT^{-2}
$\sigma_{a,s}$	surface tension air-solid	MT^{-2}
$\overline{D}$	volume average drop diameter	L
λ	mean spacing between drops	L
c	airfoil chord	L
U	flight speed	LT^{-1}
α	angle of attack	-
F	aerodynamic force on airfoil	MLT^{-2}

A Buckingham pi nondimensional analysis of these variables shows that the nondimensionalized aerodynamic force on the airofil is a function of nine nondimensional groups as follows:

$$\frac{F}{\rho_a U^2 c^2} = f(\pi_1,\ldots,\pi_9) \qquad (5)$$

where:

I. $\pi_1 = \frac{cU}{\gamma_a}$ II. $\pi_2 = \frac{cU}{\gamma_w}$

III. $\pi_3 = \frac{\rho_w U^2 D}{\sigma_{w,a}}$ IV. $\pi_4 = \frac{\sigma_{w,s}}{\sigma_{w,a}}$

V. $\pi_5 = \frac{\sigma_{a,s}}{\sigma_{w,a}}$ VI. $\pi_6 = \frac{\lambda}{c}$

VII. $\pi_7 = \frac{D}{c}$ VIII. $\pi_8 = \alpha$

IX. $\pi_9 = \frac{\rho_a}{\rho_w}$

The first two groups are simply the Reynolds numbers of the air and water respectively. The third group is the Weber number which is the ratio of inertial forces to surface tension forces. Groups four and five preserve the scaling of surface energy interaction. Groups six and seven dictate that droplet spacing and mean diameter must be scaled with the airfoil. Groups eight and nine dictate that for similar results the scaled tests must be conducted at the same angle of attack and with fluids preserving the density ratio of air to water. It is unlikely that scale model tests can be conducted while preserving all of the parameters. For example, simply increasing test velocity while decreasing model scale allows Reynolds number to remain unchanged. The Weber number, however, is a squared function of velocity and must change since the drop diameter can only be changed linearly with scale in order to preserve the seventh scaling parameter. Consequently, in order to develop the functional form for equation (5) the sensitivity of the net airfoil aerodynamic force to each of these parameters must be assessed.

It should be noted that the geometric scaling of the rain (variables six and seven) requires that liquid water content be conserved between full-scale and model-scale testing. However, since liquid water content is to be preserved in model testing, and the drop diameter is to be scaled, the distribution of drops must then be different for model testing than for full-scale testing. In natural rain the rain rate, liquid water content, and drop distribution are uniquely related. Because of drop distribution distortions due to scaling relationships rainfall rate in model testing is a less meaningful term than is liquid water content. A useful term is obtained by defining an "equivalent full-scale rainfall rate" based on the liquid water content. For most of the model test data shown the liquid water contents are quite high. In natural rain at high liquid water content most of the mass is contained in drops larger than 1 mm, and these larger drops have fall velocities from ranging 7 to 10 m/s. Since rainfall rate is the integrated product of liquid water content and drop velocity, for ease of calculation, an average drop velocity of 9 m/s was chosen and then for model tests an equivalent rainfall rate was defined as the product of LWC and the average drop velocity.

Experimental Data

Several wind tunnel tests have been conducted to explore the effect of rain on airfoils. The tests were divided amongst airfoils which had a significant amount of natural laminar flow and airfoils which had transition fixed near the leading edge. The rain effect on laminar flow airfoils will be shown to be similar to an early transition and loss of laminar flow while for conventional airfoils the rain appears to induce an early separation.

I. Rain Effects Observed During Low Reynolds Number and Laminar Flow Airfoil Tests

Pilots have reported pitch trim changes on some canard-configured sport aviation airplanes when encountering rain (reference 19). Most of these airplanes are constructed of composite materials which provide very smooth skin surfaces, and they use airfoil sections which are designed for a significant amount of natural laminar flow. NASA has tested one of these configurations (Rutan "VariEze") as a part of a general aviation stall/spin research program, and the sensitivity of longitudinal trim changes associated with early transition on the canard surface has been investigated (reference 20). Figures 10 and 11 show a full-scale model installed in the 30- by 60-Foot Wind Tunnel at the NASA Langley Research Center. For these tests the rain was sprayed only on the starboard canard surface as illustrated in figure 11 and data were collected at a freestream test velocity of 68 mph. The spray system produced a water spray quantity of 1 gal/min, which was estimated to result in a LWC of about 3.6 gm/m^3 and an equivalent rainfall rate of 4.6 inches/hour. The measured lift, drag and pitching moment on the total canard were recorded for the following conditions: (1) smooth canard surface with free transition and the water spray off, (2) a boundary-layer transition trip place along the 5-percent chord line of the entire canard, (3) smooth surface canard with free transition and the water spray on. The test results for the lift and drag on the canard surface are shown in figure 12. Fixing the transition at the 5-percent chordline caused considerable changes in the canard lift characteristics between the operating range of 2 to 16 degrees angle of attack. The water effect was only about one-half as severe as the effect of tripping the laminar boundary layer; however, the water was sprayed on only half of the canard surface. For this configuration, therefore, the effect of rain appeared to be approximately equivalent to fixing transition so that the entire chord was subject to a turbulent, rather than laminar, boundary layer.

Similar results were obtained by Hansman and Barsotti at MIT (reference 21) on a sailplane airfoil. For the tests of reference 21 a 6-inch chord Wortmann FX-67-K-170 natural laminar flow airfoil was studied in the MIT 1-Foot by 1-Foot Low-Speed Wind Tunnel. The test Reynolds number was 310,000 and the water spray had a liquid water content of 14.6 gm/M^3 corresponding to a rainfall rate of about 17.3 inches/hour. The data from reference 21 are replotted in figure 13 so that the effects of simulated rain and fixed early transition may be compared directly. The results show that the data with transition fixed at the 25-percent chord agreed fairly well with the water-spray data, but fixing the transition farther forward near the leading edge produced a more severe effect than the water spray. The work of reference 21 also showed that the degree of performance degradation was strongly dependent on the surface wetting characteristics, as illustrated in figure 14. A non-wettable surface is defined as one on which a small drop of water remains spherical and contacts the surface at only one point, whereas a fully wettable surface is defined as one in which a small drop flows to a thin uniform film. In actual practice, differing degrees of wettability fall between these two extremes. The data of figure 14 show that a waxed surface (which had the lowest degree of wettability) produced the largest lift loss and was comparable to the changes noted for fixing the transition near the leading edge as shown in figure 13.

For low Reynolds number and natural laminar flow airfoils, the wind tunnel data (references 20 and 21) and the operational experiences (reference 19) indicate that rain can act as a surface contaminant and cause early boundary-layer transition. Additionally, the sensitivity of the airfoil section to rain effects is probably dependent on the surface chemistry, specifically the wettability.

II. Rain Effects on Conventional Airfoils and High-Lift Systems

Tests on a basic airfoil section were conducted in the NASA Langley 14- by 22-Foot Subsonic Tunnel using a model wing with an NACA 0012 airfoil section. This section is similar to the types used for horizontal stabilizers on conventional general aviation aircraft. The model had a 14-inch wing chord and an aspect ratio of 8, and is shown in figure 15 immersed in water spray during a test. The tests were conducted at wind tunnel speeds ranging from 158 to 237 fps for a test Reynolds number range from 1.2×10^6 to 1.7×10^6. Transition was fixed at the 5-percent chord for all tests. Lift and drag data are shown in figure 16 for the highest test Reynolds number for liquid water contents from 13.1 to 22.2 gm/M^3. Although all spray concentrations caused about the same reduction in lift coefficient for angles of attack above 6 degrees, the measured reduction in maximum lift was not as pronounced for the lower test velocities. An increase in drag was noted for all spray concentrations at all test speeds.

The 0012 airfoil was fitted with a simple full-span trailing-edge flap having a chord equal to 30-percent of the mean aerodynamic chord. The lift and drag coefficient data for this configuration with a flap deflection of 20 degrees is shown in figure 17 for the same rainfall conditions as shown in figure 16. All three rainfall rates resulted in approximately the same amount of reduction in lift; the maximum lift coefficient was reduced about 15 percent for both the flapped wing and unflapped wing.

A cambered airfoil representative of the type used on commercial transport airplanes has also been tested in the Langley Research Center 14- by 22-Foot Subsonic Tunnel (reference 17) and is shown in figure 18. The model has an NACA 64-210 airfoil section, is of rectangular

planform, and is mounted between two end plates. The wing chord is 2-1/2 feet and the span between the end plates is 8 feet. A 1-foot span section in the center of the model is supported separately from the outer panels by an internal strain gauge balance for measuring forces and moments. The model was equipped with a leading-edge slat and a double slotted flap as shown in figure 19. Tests were conducted at wind-tunnel speeds ranging from 112 to 204 fps which resulted in model Reynolds numbers ranging from 1.8×10^6 to 3.2×10^6 based on chord length. Transition was fixed at the 5-percent chordline. The liquid water content for rain testing varied from 16 to 47 gm/m^3.

Lift and drag measurements for the basic 64-210 airfoil section model are shown in figure 20 for the highest Reynolds number tested. For these test conditions the water spray had very little effect on the lift performance, however there was an increase in drag. Tests conducted at lower Reynolds numbers actually showed a slight increase in maximum lift. The data in figure 20 for the highest Reynolds number shows a very small increase in maximum lift relative to the lower Reynolds number data. The reason for this increase is not clearly evident at present, but it is thought to be a Reynolds number effect associated with the water film on the wing increasing slightly the effective camber in the leading area of the airfoil.

For the 64-210 wing with the flaps and slat deployed, a reduction in maximum lift was measured for all test velocities and for all spray rates. A typical data set is shown for the flapped wing in figure 21. These data were taken for a wind-tunnel speed of 158 fps and for water spray concentrations of 14 to 45 gm/m^3. A sensitivity to test speed and a dependency on spray concentration were observed for this data set. Since transition was fixed on the model, the data indicate a speed sensitivity not accounted for in normal Reynolds number scaling. The dependency on spray concentration was not evident in the NACA 0012 data of figures 16 and 17. For the high lift configuration the water spray caused a reduction in maximum lift coefficient of about 20 percent and a reduction in stall angle of attack of about 8°.

Figure 22, taken from reference 22, shows the water flow on the upper surface of the wing. The photograph of figure 22 was taken at an angle of attack of 8° and 45 gm/m^3 liquid water content at a tunnel dynamic pressure of 30 lb/ft^2. The camera used for this photograph was located in the tunnel ceiling with the optical axis displaced about 18° from vertical. A thin layer with runoff streams can be seen on the aft portion of the upper surface of the wing, while the upper surface of the flap segments appear to contain higher concentrations of water than the wing. Some of the water appears to be coming from the underside of the wing through the flap gap openings. The flap mounting brackets blocked some of the flow from the underside as indicated by the nearly dry area on the flaps aft of the brackets. The results of reference 22 indicate that the water layer is thicker on the underside of the wing than on the top.

The photograph of figure 23 corresponds to the data of figure 21 and was taken with the wing at a angle of attack of 20° for a liquid water content of 45 gm/m^3 at a tunnel dynamic pressure of 30 lb/ft^2. The photograph shows that the wing had a large three-dimensional region of separated flow. The data of figure 21 shows that for a liquid water content of 45 gm/m^3 the wing was stalled beyond 12° angle of attack; whereas the data of figure 21 for the dry wing condition (0 gm/m^3) at 20° angle of attack indicate that the wing had not stalled completely. The effect of the water spray are therefore seen to be: a decrease in the maximum lift capability; an increase in drag at a given lift; and a decrease in stall angle of attack, apparently due to the water spray initiating premature flow separation.

The obtained by Hansman in reference 21, and shown in figure 14, indicate that surface wettability should be expected to be a significant factor in the degree of rain-induced lift degradation experienced by a laminar flow airfoil. Tests were conducted using the NACA 64-210 model with flaps deflected to explore the sensitivity of this type of airfoil to surface wettability effects. For these tests a surface-tension reducing agent was mixed with the water prior to injecting the water spray into the wind tunnel. Although the method used for the laminar flow airfoil investigation of wettability involved treating the wing surface, both methods change the wing surface/water interface interaction by altering the surface tension. The lift and drag data for the high-lift configuration with the surface tension reduced by a factor of two by the reducing agent are shown in figure 24. When comparisons are made between the data for the high-lift configuration with and without the surface tension reducing agent (compare figure 21 with figure 24), there is no apparent dependency on surface tension. It appears, therefore, that the sensitivity to scaling variables may be different for rain-induced effects on laminar flow airfoils as compared to turbulent boundary layer, high-lift configured airfoils.

Summary Remarks

In the past six years, considerable effort has been directed at investigating both analytically and experimentally the influence of rain on airfoil performance. From model data and actual flight experiences, airplanes with natural laminar flow lifting surfaces have been observed to experience performance changes associated with rain encounters that are nearly equivalent to a loss in laminar flow. The influence of rain on more conventional airfoils with and without high lift devices is as yet unresolved.

A conventional NACA 64-210 airfoil and an unflapped NACA 0012 airfoil displayed different sensitivities to a simulated rain spray. The NACA 0012 showed a loss in maximum lift capability while very little effect was noted on the lift of the NACA 64-210 airfoil. With both airfoils in a flapped configuration significant

reductions in maximum lift capability were noted. Additionally, for the NACA 64-210 airfoil a significant reduction in angle of attack for maximum lift was observed. For both airfoils, the effect of rain on lift occured near the region of maximum lift and little effect was observed at lower angles of attack.

Scaling laws have not yet been well established for extrapolating model results to full scale. However, if the results shown for a conventional airfoil in a high-lift configuration are directly applicable to full scale airplanes, then rain would present an operational hazard which has previously not been considered. Specifically, performance margins for coping with adverse conditions (such as windshears) during landing and take-off are based on dry air performance data, and these performance margins may be significantly reduced in heavy rain. A determination of the influence of rain on a full size airplane is required to provide safe piloting procedures for escaping from a windshear in a rain environment, and for determining the windshear magnitudes which must be avoided.

Considerable analytical and experimental work is required to understand fully the significance of the various mechanisms involved in the generation of lift in a two-component, two-phase flow. Large-scale data will be required for validating scaling laws which may be developed analytically or experimentally. Additionally, large-scale data may be required because the scaling may prove to be so complex that small-scale data cannot be extrapolated with confidence.

In recognition of the requirement for large scale data, the NASA Langley Research Center is planning to conduct a test on a large-chord wing model. The airfoil will be placed on top of a large carriage towing-type facility. The carriage to be used is known as the Aircraft Landing Dynamics Facility (ALDF) and is currently used for landing gear and tire studies. The carriage with the attached wing will be capable of test speeds of up to 170 kts. A portion of the approximately 750-meter test track will be equipped with a rain spray simulation system capable of simulated rain rates from 50 mm/hr to greater than 1000 mm/hr.

References

1. Marshall, J. S. and Palmer, W. McK.: The Distribution of Raindrops with Size. Journal of Meteorology, Volume 5, 1948, pg. 165-166.

2. Joss, J. and Waldvogel, A.: Raindrop Size Distribution and Sampling Size Errors. Journal of the Atmospheric Sciences, Volume 3, 1969, pg. 566-569.

3. Markowitz, Allan H.: Raindrop Size Distribution Expressions. Journal of Applied Meterology, Volume 15, September, 1976, pg. 1029-1030.

4. Riordan, P.: Weather Extremes Around the World. Earth Sciences Laboratory, TR-70-45-ES, January 1970.

5. Jones, D. M. A. and Sims, A. L.: Climatology of Instantaneous Rainfall Rates. Journal of Applied Meterology, Volume 17, August 1978, pg. 1135-1140.

6. Roys, George P. and Kessler, Edwin: Measurements by Aircraft of Condensed Water in Great Plains Thunderstorms. National Sever Storms Laboratory Publication. TN-49-NSSP-19, 1966.

7. Rhode, Richard V.: Some Effects of Rainfall on Flight of Airplanes and on Instruemnt Indications. NACA TN803, April 1941.

8. Haines, P. A. and Luers, J. K.: Aerodynamic Penalties of Heavy Rain on a Landing Airplane. NASA CR 156885, July 1982.

9. Bergrun, Norman R.: A Method of Numerically Calculating the Area and Distribution of Water Impingement on the Leading Edge of an Airfoil. NACA TN1397, 1947.

10. Bergrun, Norman, R.: An Empirically Derived Basis for Calculating the Area, Rate, and Distribution of Water-Drop Impingement on Airfoils. NACA Report 1107, 1952.

11. Dorsch, R. G. and Brun, R. J.: A Method for Determining Cloud-Droplet Impingement on Swept Wings. NACA TN2931, 1953.

12. Morsi, S. A., and Alexander, A. J.: An Investigation of Particle Trajectories in Two-Phase Flow Systems. Journal of Fluid Mechanics, Volume 56, 1972, page 193-208.

13. Bragg, M. B.: A Similarity Analysis of the Droplet Trajectory Equation. AIAA Journal, Volume 20, December 1982, pg. 1681-1686.

14. Calarese, W. and Hankey, W. L.: "Numerical Analysis of Rain Effects on an Airfoil," AIAA-84-0539, AIAA 22nd Aerospace Sciences Meeting, Reno, NV, January 1984.

15. Kisielewski, Keith: A Numerical Investigation of Rain Effects on Lift using a Three-Dimensional Split Flux Vector Form of the Euler Equations, Master Thesis, Department of Aerospace Engineering, Mississippi State University, May 1985.

16. Feo, A.: Single Drop Impact Studies, AIAA 8-0257, AIAA 25th Aerospace Sciences Meeting, Reno, NV, January 1987.

17. Dunham, R. E., Jr.; Bezos, G. M.; Gentry, G. L., Jr.; and Melson, E. M., Jr.: "Two-Dimensional Wind Tunnel Tests of a Transport-Type Airfoil in a Water Spray," AIAA-85-0258, AIAA 23rd Aerospace Sciences Meeting, Reno, NV, January 1985.

18. Bilanin, A. J.: "Scaling Laws for Testing of High Lift Airfoils Under Heavy Rainfall," AIAA-85-0257, AIAA 23rd Aerospace Sciences Meeting, Reno, NV, January 1985.

19. Dwiggins, D.: Dangerous When Wet? Homebuilt Aircraft, March 1983.

20. Yip, L. P.: Wind-Tunnel Investigation of a Full-Scale Canard-Configured General Aviation Airplane. NASA TP-2382, March 1985.

21. Hansman Jr., R. J.; and Barsotti, M. F.: The Aerodynamic Effect of Surface Wetting Characteristics on a Laminar Flow Airfoil in a Simulated Heavy Rain. AIAA 85-0260, January 1985.

22. Hastings, Earl C., Jr. and Manuel, Gregory S.: Measurements of Water Film Characterisitcs on Aircraft Surfaces from Wind Tunnel Tests," AIAA 85-0259, January 1985.

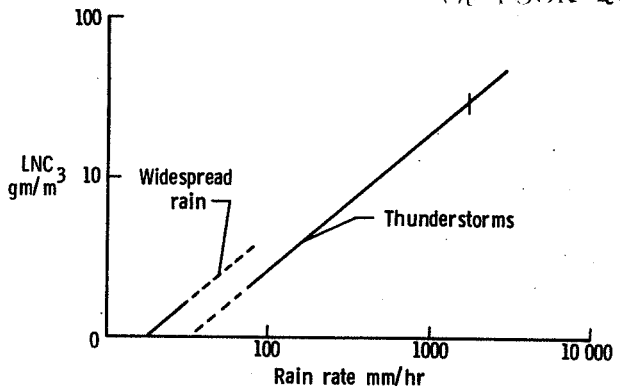

Figure 1. Liquid water content as a function of rain rate.

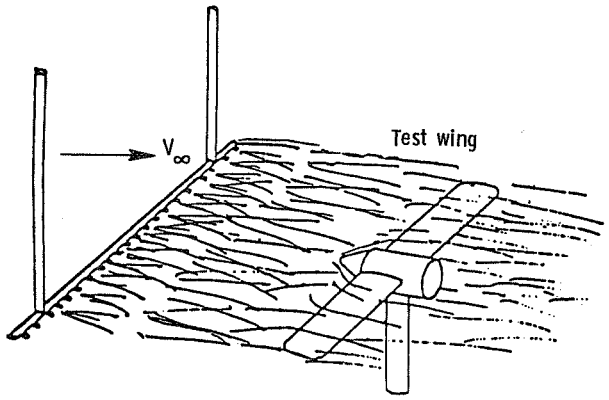

Figure 4. Typical wind-tunnel tests set-up for simulated rain effects studies.

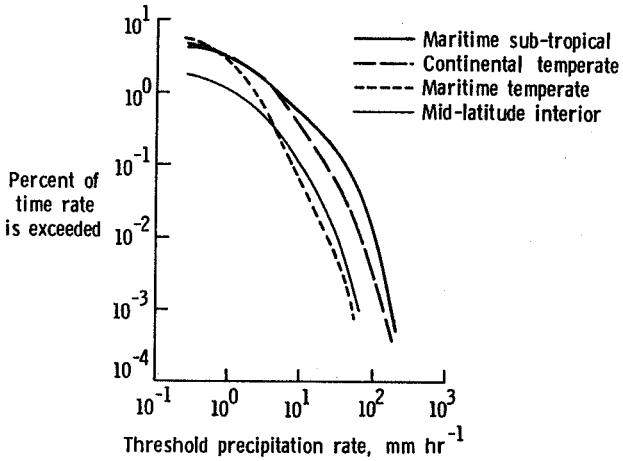

Figure 2. Average rainfall rate-frequency relationship for four rain climates.

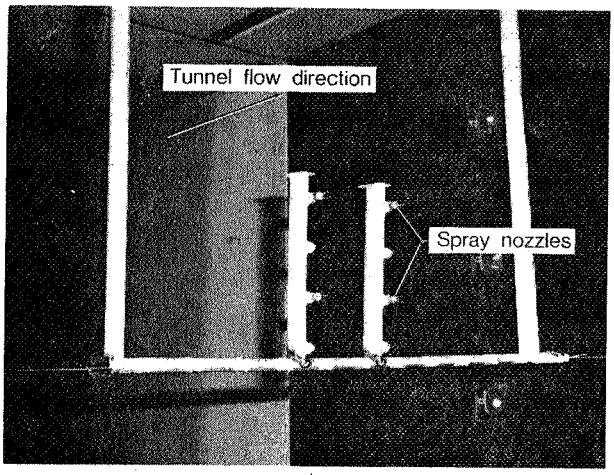

Figure 5. Spray mainfold for wind-tunnel rain simulation.

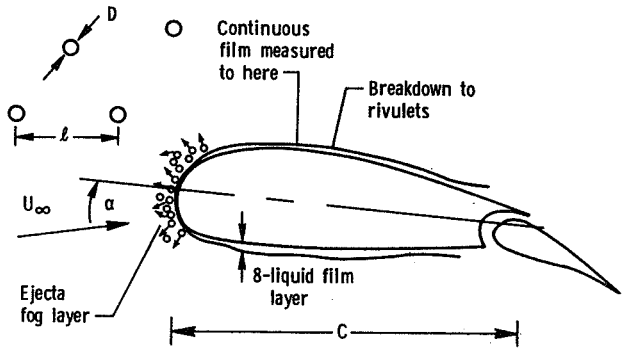

Figure 3. Illustration of rain drops interacting with an airfoil.

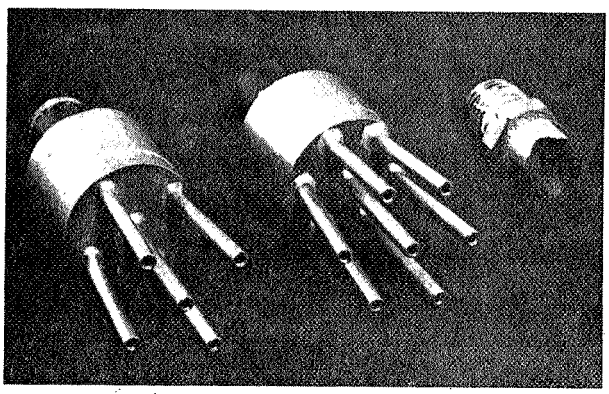

Figure 6. Three nozzles used to vary the water spray characteristics. From left to right: 5-tube, 7-tube, and commercial nozzle.

$RR_e = LWC \cdot W_d$

$LWC = \frac{\dot{M}}{V_\infty WH}$

RR_e = Rainfall Rate
LWC = Liquid Water Content
W_d = Rain Fall Velocity
W = Spray Width at Model
H = Spray Height at Model
V_∞ = Freestream Velocity
$\dot{M}$ = Water Mass Flow in Spray Bar

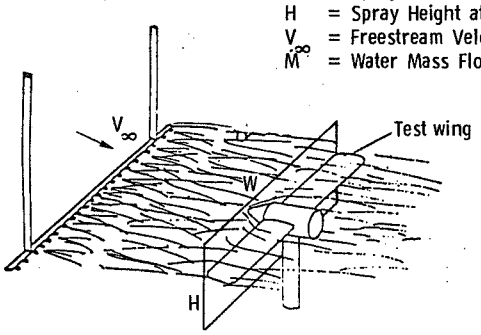

Figure 7. An illustration of the method for determining liquid water content during wind-tunnel tests.

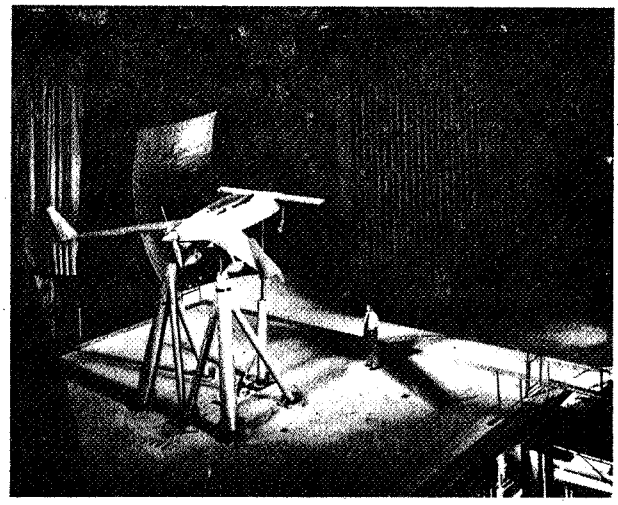

Figure 10. Vari Eze airplane in the Langley Research Center 30- by 60-Foot Wind Tunnel.

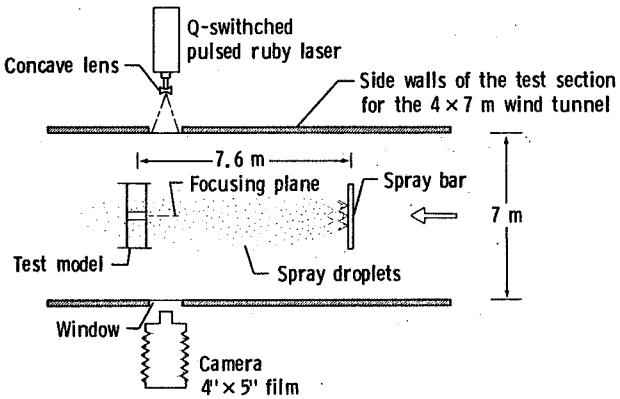

Figure 8. A sketch of the set-up for calibrating the spray pattern during wind-tunnel tests.

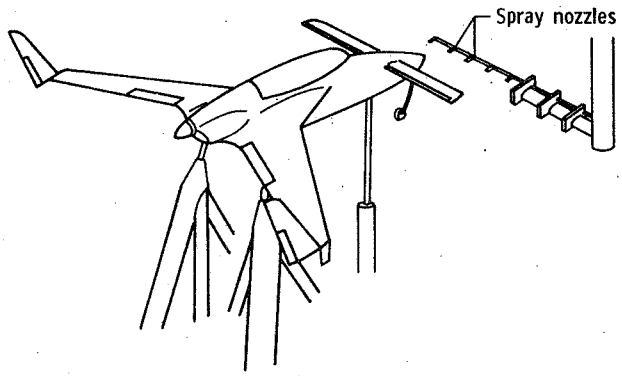

Figure 11. Illustration of spray nozzle system used for Vari Eze canard study.

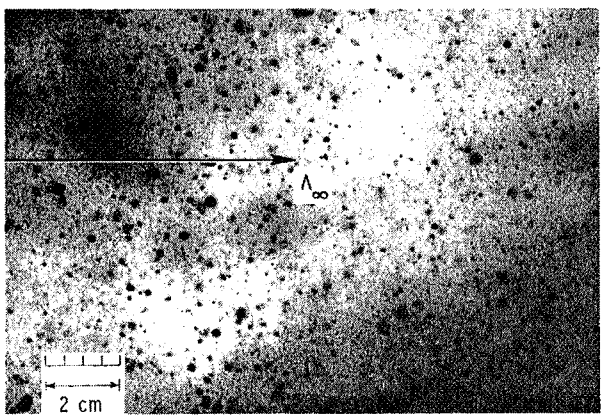

Figure 9. A typical shadowgraph photo taken for spray calibration.

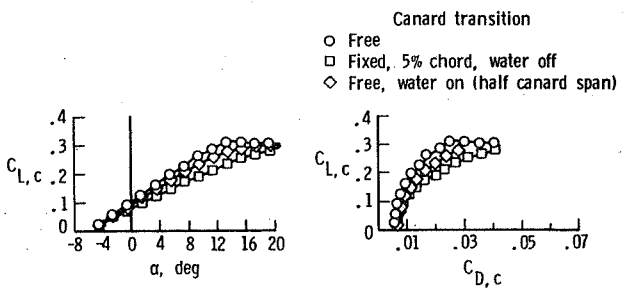

Figure 12. Canard tests data (reference 20).

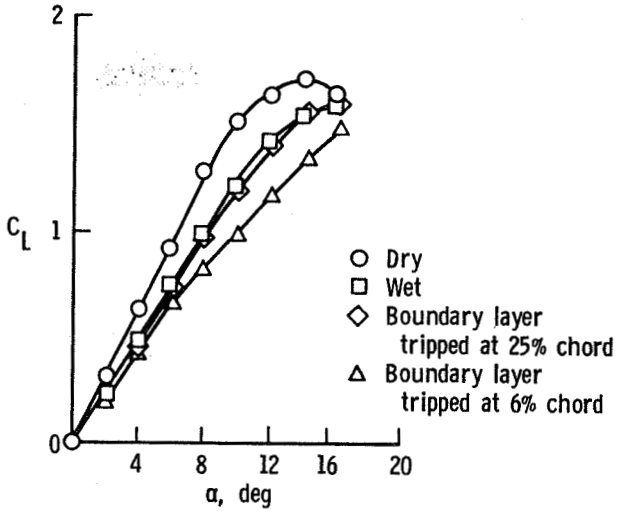

Figure 13. Comparison of water effects with fixed transition for a low Reynolds number natural laminar flow airfoil (reference 21).

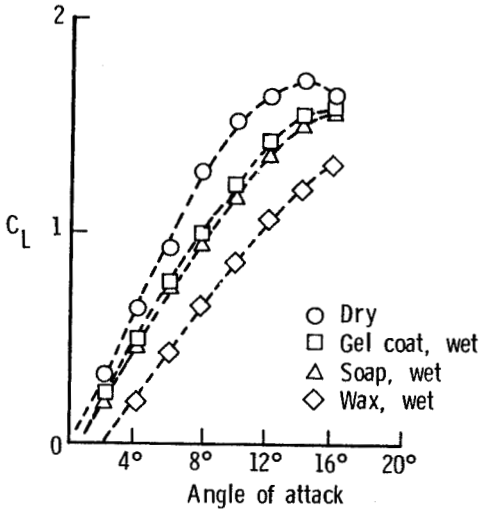

Figure 14. The effect of surface wettability on the performance changes associated with a water spray on a low Reynolds number natural laminar flow airfoil (reference 21).

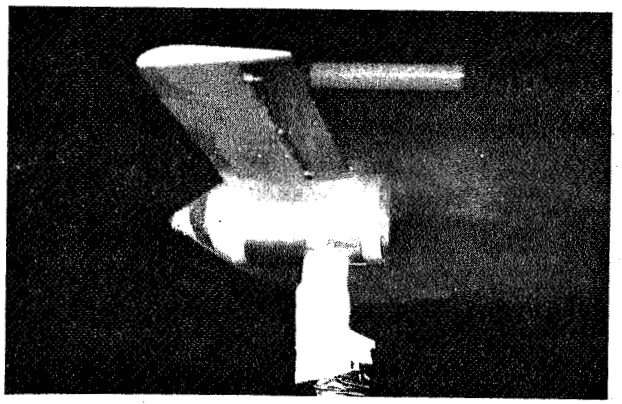

Figure 15. Photograph of NACA 0012 wing model immersed in a water spray.

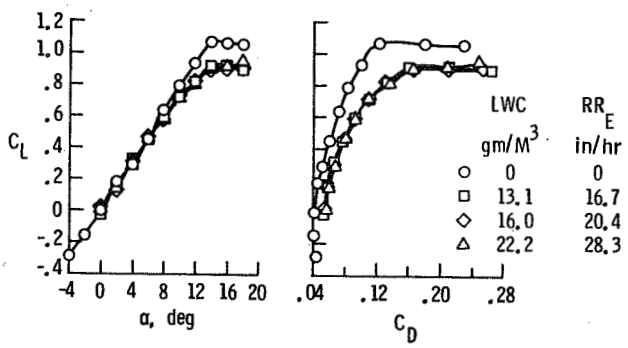

Figure 16. Lift and drag measurements on a NACA 0012 wing model subjected to several water spray concentrations.

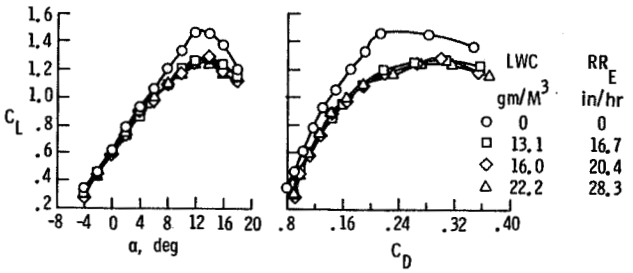

Figure 17. Lift and drag measurements on a NACA 0012 wing model with a 30% chord flap deflected 20° while subjected to several water spray concentrations.

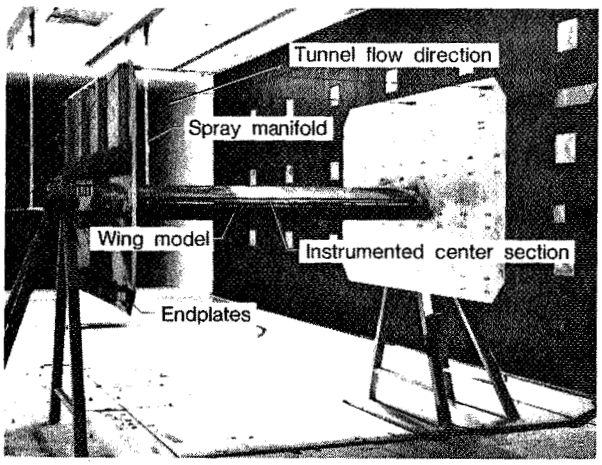

Figure 18. Photograph of NACA 64-210 airfoil model installed in the NASA Langley 14- by 22-Foot Subsonic Tunnel.

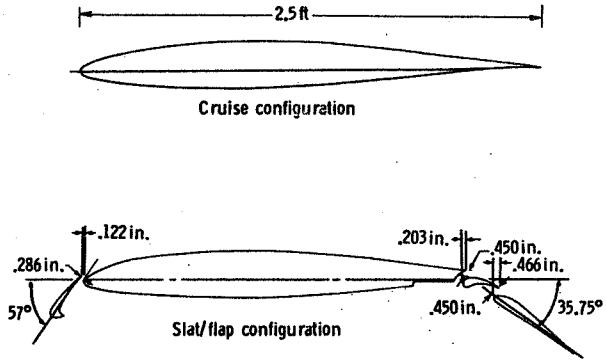

Figure 19. Cross section of NACA 64-210 airfoil model and details of slat and flap installation.

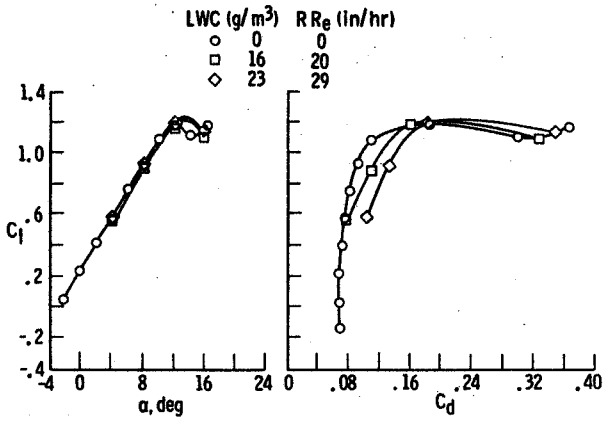

Figure 20. Lift and drag measurements on a NACA 64-210 wing model while subjected to several water spray concentrations.

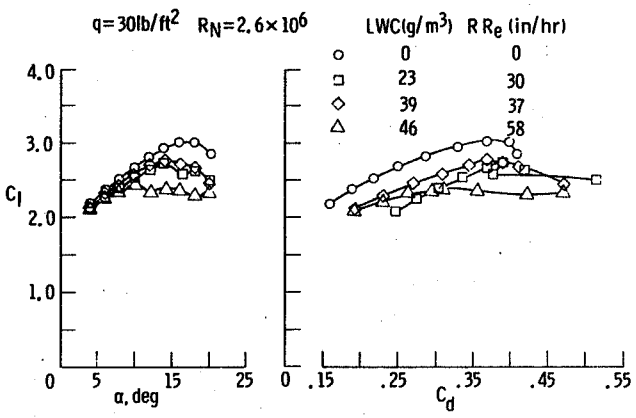

Figure 21. Lift and drag data for the high-lift configuration at a dynamic pressure of 30 lb/ft^2.

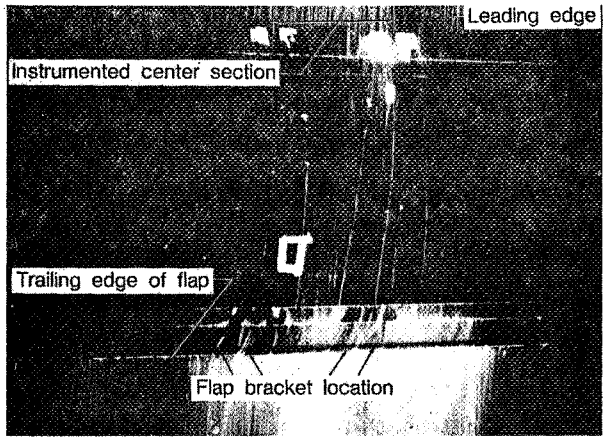

Figure 22. Water film pattern on wing upper surface for the flap/slat configuration at an angle of attack of 8°, a tunnel dynamic pressure of 30 lb/ft^2 and a liquid water content of 45 gm/m^3.

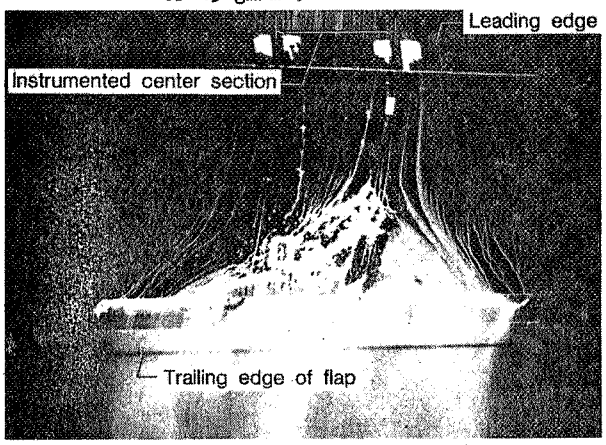

Figure 23. Water film pattern on wing upper surface for the flap/slat configuration at an angle of attack of 20°, a tunnel dynamic pressure of 30 lb/ft^2 and a liquid water content of 45 gm/m^3.

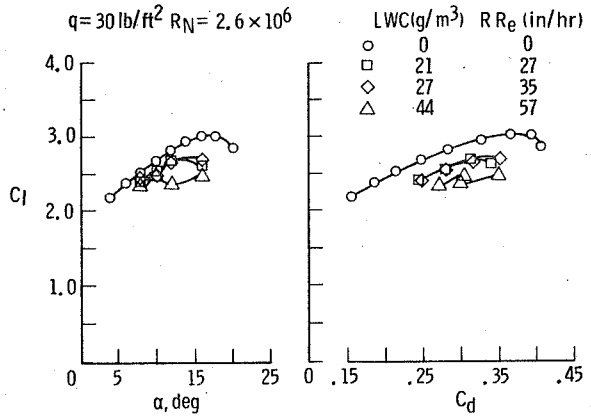

Figure 24. Lift and drag measurements at a dynamic pressure of 30 lb/ft^2 for the high-lift configuration immersed in a water spray containing a surface tension reducing agent.